GLIA 54:135–145 (2006)

A Dual Tyrosine-Leucine Motif Mediates Myelin Protein P_0 Targeting in MDCK Cells

GRAHAME J. KIDD,[1]* VIJAY K. YADAV,[1] PING HUANG,[1] STACEY L. BRAND,[1] SENG HUI LOW,[2] THOMAS WEIMBS,[2] AND BRUCE D. TRAPP[1]

[1]*Department of Neurosciences, Lerner Research Institute, Cleveland Clinic Foundation, Cleveland, Ohio*
[2]*Department of Molecular, Cellular, and Developmental Biology, University of California Santa Barbara, Santa Barbara, California*

KEY WORDS
myelin; protein targeting; protein sorting; membrane assembly; Schwann cells

ABSTRACT
Differential targeting of myelin proteins to multiple, biochemically and functionally distinct Schwann cell plasma membrane domains is essential for myelin formation. In this study, we investigated whether the myelin protein P_0 contains targeting signals using Madin-Darby canine kidney (MDCK) cells. By confocal microscopy, P_0 was localized to MDCK cell basolateral membranes. C-terminal deletion resulted in apical accumulation, and stepwise deletions defined a 15-mer region that was required for basolateral targeting. Alanine substitutions within this region identified the YAML sequence as a functional tyrosine-based targeting signal, with the ML sequence serving as a secondary leucine-based signal. Replacement of the P_0 ectodomain with green fluorescent protein altered the distribution of constructs lacking the YAML signal. Coexpression of the myelin-associated glycoprotein did not alter P_0 distribution in MDCK cells. The results indicate that P_0 contains a hierarchy of targeting signals, which may contribute to P_0 localization in myelinating Schwann cells and the pathogenesis in human disease.

INTRODUCTION

Schwann cell myelination represents an evolutionary highpoint in the cell biology of membrane production. Formed by extension of the Schwann cell plasma membrane, myelin membranes may extend 2 mm between nodes and wrap around the axon with a spiral length that may be 2–3 times that length (Thomas et al., 1993). Although contiguous with the external plasma membrane, myelin membranes are partitioned into distinct domains that have very different compositions and functions (see Arroyo and Scherer, 2000; Sherman and Brophy, 2005; Trapp et al., 2004; Trapp and Kidd, 2004). Compact myelin membranes exhibit close extracellular and intracellular spacings, mediated largely by the obligate homophilic adhesion molecule, P_0 (*mpz* gene Giese et al., 1992; Shapiro et al., 1996). Noncompact membrane domains include the paranodal loops, Schmidt-Lanterman incisures, and periaxonal membranes, which contain the myelin-associated glycoprotein (MAG), and lack P_0 (Trapp and Quarles, 1982) and other compact myelin proteins. Membranes of the paranodal loops are also enriched for junctional proteins that permit intra-Schwann cell junctions and Schwann cell-axon junctions (reviewed by Arroyo and Scherer, 2000; Pedraza et al., 2001; Sherman and Brophy, 2005; Trapp et al., 2004). The outer (abaxonal) Schwann cell plasma membrane domain is specialized for extracellular interactions and contains integrins, proteoglycans, and cytoskeletal proteins while lacking other myelin membrane proteins such as P_0 and MAG (Arroyo and Scherer, 2000; Sherman and Brophy, 2005; Trapp and Kidd, 2004). Formation and maintenance of myelin internodes are dependent on the timely production and assembly of components in each of these domains. Increased or decreased expression of proteins from compact myelin (Valentijn et al., 1992; Yin et al., 2000), noncompact membranes (Yin et al., 1997, 1998) or the outer membrane (Feltri et al., 2002; Sherman et al., 2001) results in dysmyelination or myelin instability that cause substantial human neuropathological disability (Kamholz et al., 2000; Scherer, 1999; Shy et al., 2004; Wrabetz et al., 2004).

Protein transport and targeting mechanisms play a major role in myelin membrane assembly. Microtubules are essential for millimeter-scale protein trafficking along the myelin internode (Trapp et al., 1995), and Schwann cells establish specialized microtubule networks during myelination to accommodate the high biosynthetic demands of myelination (Kidd et al., 1994, 1996). Sorting in the trans-Golgi network (TGN) partitions P_0 and MAG into separate transport vesicles (Trapp et al., 1995). P_0- and MAG-containing vesicles do not fuse with each other or with incompatible Schwann cell membranes (Trapp et al., 1995), indicating that vesicle docking and fusion are tightly regulated. These features largely explain why P_0 and MAG are never normally detected in the same membranes (Trapp and Quarles, 1982). P_0 overexpression in a transgenic mouse also resulted in P_0 mistargeting to

Grant sponsor: National Institute of Health; Grant number: NS38186.

*Correspondence to: Grahame Kidd, Ph.D., Department of Neurosciences-NC30, Cleveland Clinic-Lerner Research Institute, 9500 Euclid Avenue, Cleveland, Ohio 44195, USA. E-mail: kiddg@nue.org

Received 17 February 2006; Accepted 26 April 2006

DOI 10.1002/glia.20366

Published online 20 June 2006 in Wiley InterScience (www.interscience.wiley.com).

all Schwann cell membranes and resulted in arrested myelination through P_0–P_0 interactions preventing mesaxon spiral elongation (Yin et al., 2000). Mistargeting of P_0 and MAG to the same mesaxonal membranes is observed in the trembler mouse (Heath et al., 1991), an animal model for Charcot-Marie-Tooth disease, suggesting that protein mistargeting may be a component of human pathology.

At a molecular level, it is unknown by what basis P_0 is recognized for sorting in the TGN or targeted to compact myelin, although several possibilities have been proposed. Compact myelin is enriched for cholesterol and glycosphingolipids (Norton and Cammer, 1984), characteristic of lipid rafts. Association of P_0 with lipid rafts in TGN membranes could thus promote targeting to compact myelin. Raft-association could potentially occur through P_0 acylation, which occurs on C^{153} (Gao et al., 2000; Zhang and Filbin, 1998), or through transmembrane domain interactions. Self-association of P_0 tetramers (Inouye et al., 1999; Shapiro et al., 1996) might potentially generate P_0-enriched membrane microdomains that spontaneously segregate P_0 from other transmembrane proteins. Homophilic adhesion in trans (between membranes) may also stabilize and concentrate P_0 in apposing target membrane, as observed in some cultured cells (D'Urso et al., 1990; Filbin et al., 1990). In other polarized cell systems, peptide motifs within the cytoplasmic domain frequently direct protein targeting to particular cell surfaces (Matter and Mellman, 1994; Mostov et al., 2005; Nelson and Yeaman, 2001), and extracellular glycosylation can also contribute to protein targeting.

Identifying P_0 targeting motifs in myelinating Schwann cells is difficult, because mutations that disrupt P_0 adhesion may produce similar phenotypes to those affecting targeting. As P_0 is the principal compact myelin protein, alterations in its distribution during initial myelination can also block Schwann cell membrane polarization and prevent other myelin membrane domains from forming (Yin et al., 2000). Targeting mechanisms are often conserved among otherwise highly divergent cell types, as shown for epithelial cells and neurons (de Hoop and Dotti, 1993; Silverman et al., 2005). In this study, we have investigated whether P_0 contains targeting signals using Madin-Darby canine kidney (MDCK) cells as a model system. MDCK cells are ideally suited for this purpose because they are an easily transfected cell line that polarizes into two membrane domains. Proteins are targeted through a variety of mechanisms involving peptide motifs, post-translation modifications, and lipid raft-associations (Mostov et al., 2000, 2005; Weimbs et al., 1997; Yeaman et al., 1999). This approach has been used to study other myelin proteins (Kroepfl and Gardinier, 2001; Minuk and Braun, 1996), as it obviates practical problems of cell-specific protein interactions and interpretation of complex membrane morphologies of myelinating cells. Using this approach, we have identified several candidate targeting signals in P_0, including a novel motif that includes active tyrosine-based and leucine-based signals.

MATERIALS AND METHODS

Materials and Antibodies

P_0 was detected by immunostaining using rabbit polyclonal antibodies (Trapp and Quarles, 1982). MDCK cell surfaces were labeled with mouse monoclonal antibodies against GP135 (apical) or p58 (antibody 6.23.23; basolateral), as previously described (Low et al., 1998). Internal organelles were labeled using mouse monoclonal antibodies against LAMP-2 (lysosomes; AC17 antibody), EEA1 (endosomes; BD Biosciences, San Jose, CA), transferrin receptor (endosomes; CHEMICON, Temecula, CA), and Golgin97 protein (Molecular Probes, Eugene, OR). Mouse monoclonal antibodies (CHEMICON) were used to stain MAG, both L-and S-isoforms; rabbit L-MAG specific antibodies (Bö et al., 1995) were used for Western blots. Secondary antibodies raised in donkey and directed against rabbit, mouse, and rat immunoglobulins (Jackson Immunobiologicals, Bar Harbor, MN) were directly conjugated to either FITC or TexasRed. Unless specified, all other reagents were purchased from Sigma-Aldrich (St Louis, MO).

Generation of P_0 Constructs

Full length rat P_0 cDNA was provided by Dr. David Colman (accession number NM_017027.1). Constructs based on this cDNA were generated by PCR using Pfu DNA polymerase (Stratagene, La Jolla CA) and the resulting PCR products were gel purified, digested, and ligated into the multiple cloning site of pcDNA4/T0 (Invitrogen, Carlesbad, CA). This vector allows tetracycline-regulated expression of the cloned gene in mammalian host cells co-transfected with pcDNA6/TR (Invitrogen). Cloning was carried out in super-competent XL1-Blue MRF' cells (Stratagene), and plasmid DNA harvested using QIAGEN endofree maxiprep kit (QIAGEN, Valencia CA). Constructs were confirmed by sequencing by the Cleveland Clinic Foundation DNA Sequencing Core Facility.

Figure 1 shows the constructs generated in this study, using amino acid numbering based on the mature peptide (i.e. not including the signal peptide). For full length P_0, a PCR fragment including the P_0 coding region, 5′ untranslated region (UTR), and most of the 3′UTR was amplified, and 5′ HindIII and 3′ BamHI restriction sites were introduced, using the primers shown in Table 1. Truncations in which the C-terminal was progressively removed were generated using the same forward primer, and reverse primers for P_0-TMD (i.e. R^{151}-stop), $P_0\Delta15$ (i.e. S^{204}-stop), $P_0\Delta30$ (i.e. V^{189}-stop), $P_0\Delta45$ (i.e. F^{173}-stop) and $P_0\Delta60$ (i.e. L^{155}-stop) as listed in Table 1.

P_0 constructs with alanine substitutions for Y^{152}, Y^{191}, M^{193}, L^{194}, singly and in combinations, were generated initially as two overlapping PCR fragments. The 3′ end of fragment 1 (upstream sequence) and 5′ end of fragment 2 (downstream sequence) were complementary and contained the engineered base changes; primers used are shown in Table 1. Fragments 1 and 2 were purified, annealed together, and the final construct produced by PCR using the forward primer for fragment 1 and the reverse primer for fragment 2.

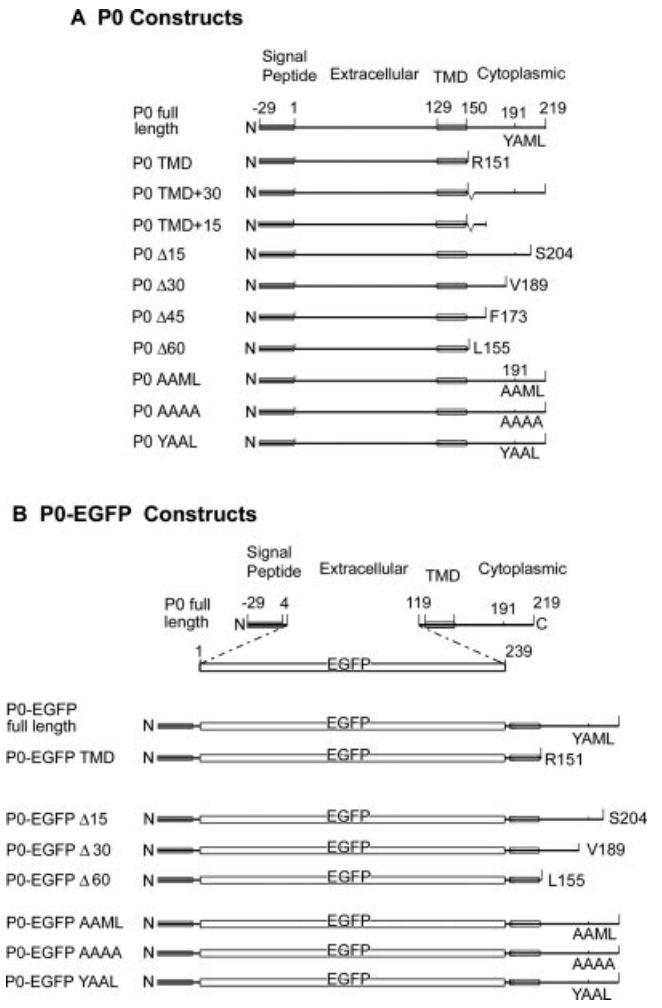

Fig. 1. P_0 constructs generated in this study. Amino acids are numbered as in the mature peptide (i.e not including the cleaved signal peptide).

Two constructs were generated in which amino acids between L^{155} and either L^{190} (construct P_0-TMD+30) or E^{205} (construct P_0-TMD+15) were removed. Two PCR fragments were initially generated for each construct in which the 3′ end of fragment 1 and the 5′ end of fragment 2 were complementary and included codons upstream and including L^{155}, and downstream and including L^{190} or E^{205} (see Table 1 for primer pairs). The final construct was generated by annealing fragments 1 and 2, then performing PCR using the forward primer for fragment 1 and the reverse primer for fragment 2.

In several constructs, the extracellular domain of P_0 was deleted between Y^4 and E^{119}, and the entire sequence of enhanced green fluorescent protein (EGFP) inserted. These constructs were generated as three fragments. One fragment encompassed the P_0 5′UTR and codons for the signal sequence through to D^5. A second DNA encompassed all of the EGFP sequence using pEGFP-N1 (BD Biosciences) as a template. Fragments 1 (300 bp) and 2 (700 bp) contained overlapping 3′ and 5′ (respectively) regions, and PCR of annealed fragments 1 and 2 using forward primer 19 (Table 1) and reverse primer 20 produced a cDNA encoding P_0 5′UTR signal sequence and first 5 amino acids spliced to the EGFP protein. A third set of PCR products was generated that encoded P_0 from L^{155} into the 3′UTR (primers, Table 1), with a 5′ overhang that complemented the EGFP 3′ end. Control and mutated forms of this segment were generated by using the mutated P_0 constructs (above) as PCR templates for this step. When annealed to fragments from steps 1 and 2, these produced a DNA encoding the P_0 5′UTR, signal sequence to D^5, EGFP, the P_0 transmembrane domain, and the P_0 cytoplasmic domain with several mutations or truncations (Fig. 1). All of these P_0-EGFP constructs were ligated into the pcDNA4/T0 vector, maxipreped, and confirmed by sequencing, as described above.

Cell Culture and Transfection

Untreated Madin Darby Canine kidney (MDCK II) cells were grown from stocks maintained in liquid nitrogen, and expanded at 37°C in a 5% CO_2 atmosphere in MEM (Invitrogen) supplemented with 10% fetal bovine serum (Invitrogen), 100 U/mL penicillin, and 100 μg/mL streptomycin.

For transfection, the cells were plated at high density onto 6-well Falcon tissue culture plates and grown to 60–80% confluence in overnight. They were transfected using ExGen500 (Fermantas, Hannover MD). For one well, 6.6 μL of ExGen500 was combined with 2 μg of the construct DNA in 100 μL of 0.15 M NaCl and incubated at room temperature for 10 min. The DNA/ExGen mixture was then combined with MDCK Cells in serum-reduced opti-MEM medium (Invitrogen) were incubated for 2 h at 37°C. After growing for 6 h, the cells were plated onto Transwell polycarbonate filters (12 mm, 0.4 μm pore size, Corning Costar, Cambridge, MA) and allowed to grow and polarize on the membrane filters for up to 60 h in the incubator. In experiments using the Tet repressor-expressing cells, gene expression was derepressed by addition of doxycyclin (Invitrogen) after 24 h.

For initial experiments using full length P_0, P_0-TMD, and L-MAG or S-MAG (constructs generously provided by Dr Peter Braun), stably transfected cell lines were generated from MDCK II stock cells, as previously described (Low et al., 1996). Briefly, the cells were transfected, and allowed to grow in medium for 2 days. Cells were then switched to kanamycin-containing medium (Invitrogen), and grown for a further 2 days. Resistant cells were then dissociated, diluted, and allowed to grow up as single clones in large culture dishes. Twenty clones were selected from each experiment, grown to high density and Western blotted to detect those cells expressing the transfected protein. High expressing clones were then propagated and stored in liquid nitrogen until required.

Immunostaining and Confocal Imaging

All steps were carried at room temperature. PBS contained 100 μM each of $CaCl_2$ and $MgCl_2$ unless stated

TABLE 1. Primer Pairs Used in PCR Generation of P_0 Constructs

Construct	Pr no.	Forward	Reverse
Full P_0	1	GCCCAAGCTTCTACCCCAGCTATGGCTCCT	GCGCGGATCCCTATTTCTTATCCTTGCGAG
P_0-TMD	2	GCCCAAGCTTCTACCCCAGCTATGGCTCCT	TCTTCTCCAGCCAGCAGGCCCGGATCAG
$P_0\Delta15$	3	GCCCAAGCTTCTACCCCAGCTATGGCTCCT	TTCTGGATCCCTAACTGGCAGCTTTGGTGC
$P_0\Delta30$	4	GCCCAAGCTTCTACCCCAGCTATGGCTCCT	TCTTGGATCCCTACACTGGCGTCTGCCGCC
$P_0\Delta45$	5	GCCCAAGCTTCTACCCCAGCTATGGCTCCT	TCTTGGATCCCTACTGAAATTTCCCCTTCTC
$P_0\Delta60$	6	GCCCAAGCTTCTACCCCAGCTATGGCTCCT	GATTGGATCCCTACAGCCAGCAGTACCGGA
P_0 Y152A			
Frag 1	7	GCCCAAGCTTCTACCCCAGCTATGGCTCCT	CTGCGCAGCCAGCAGGCCCGGATCAGGTA
Frag 2	8	TACCTGATCCGGGCCTGCTGGCTGCGCAG	GCGCGGATCCCTATTTCTTATCCTTGCGAG
P_0-Y191A			
Frag 1	9	GCCCAAGCTTCTACCCCAGCTATGGCTCCT	CTGTGGTCCAGCATGGCGGCCAGCACTGGC
Frag 2	10	GCCAGTGCTGGCCGCCATGCTGGACCACAG	GCGCGGATCCCTATTTCTTATCCTTGCGAG
P_0-M193A			
Frag 1	11	GCCCAAGCTTCTACCCCAGCTATGGCTCCT	CAGTGCGGCATACAGCACTGGCGTCTGCC
Frag 2	12	TATGCCGCACTGGACCAGAGCCGAAGCAC	GCGCGGATCCCTATTTCTTATCCTTGCGAG
P_0-AAAA			
Frag 1	13	GCCCAAGCTTCTACCCCAGCTATGGCTCCT	TGCTGCGGCTGCCAGCACTGGCGTCTGCCG
Frag 2	14	GCAGCCGCAGCAGACCACAGCCGAAGCACCA	GCGCGGATCCCTATTTCTTATCCTTGCGAG
P_0-TMD+15			
Frag 1	15	GCCCAAGCTTCTACCCCAGCTATGGCTCCT	TCTTCTCCAGCCAGCAGGCCCGGATCAG
Frag 2	16	TGCTGGCTGGAGAAGAAATCTAAAGGGCTG	GCTCCGAGCTCTGCTCATCTTTGCGAAG
P_0-TMD+30			
Frag 1	17	GCCCAAGCTTCTACCCCAGCTATGGCTCCT	GGCATACAGCAGGGCAGCCTGCCTGCGCAG
Frag 2	18	GCTGCCCTGCTGTATGCCATGCTGGACCA	GCTCCGAGCTCTGCTCATCTTTGCGAAG
P_0 5' (Frag 1)	19	CGCAATGGGCGGTAGGCGTGTACGGTG	GCTCAGCATGTCCGTGTAAACCACAATG
EGFP-N1 (Frag 2)	20	TACACGGACATGGTGAGCAAGGGCGAGGAGC	CACTTTTTCCTTGTACAGCTCGTCCATGC
P_0 3' (Frag 3)	21	CTGTACAAGGAAAAAGTGCCCACTAGGTA	GCGCGGATCCCTATTTCTTATCCTTGCGAG
P_0-EGFP assembly	22	CGCAATGGGCGGTAGGCGTGTACGGTG	GCGCGGATCCCTATTTCTTATCCTTGCGAG

See Materials and Methods for detailed explanation of construct assembly.

otherwise. Cells on membranes in transwell inserts were washed with chilled PBS and fixed with 4% paraformaldehyde in PBS for 20 min. After washing with PBS, they were quenched with 75 mM NH_4Cl and 20 mM glycine in PBS for 10 min. Cells were then washed three times in PBS before incubating with a blocking/permeabilization solution containing 10% fetal bovine serum, 0.2% Triton X-100, and 0.05% sodium azide in PBS for 30 min at 37°C. The cells transfected with P_0 constructs were immunostained with primary antibodies for P_0 (rabbit polyclonal, (Trapp et al., 1981) and mouse monoclonal antibodies for markers of apical (GP135) or basolateral (P58) surfaces. The cells transfected with P_0 constructs containing reporter protein EGFP were stained with surface marker antibodies only. Cells were washed three times, and incubated with secondary antibodies applied for 1 h at 37°C in a humidified chamber. After repeated washing, the filters were excised from the transwell supports using a scalpel and mounted on slides with Vectashield (Vectorlabs, Burlingame, CA).

The cells were imaged with a Leica TCS-NT confocal microscope (Leica Microsystems, Exton PA) equipped with 40×, 1.25 NA and 63×, 1.4 NA lenses. Cells were imaged in the *XZ* plane, though some areas were images in the *XY* plane or as *XYZ* series. Only completely polarized cells were examined, as apical and basolateral proteins can have mixed distributions prior to complete polarization. For transient transfections, a minimum of 50 polarized transgene-expressing cells was examined for each construct. Images were viewed using Scion Image (Scion Corporation, Frederick, MD) or Leica Confocal software (Leica) and assembled for production in Adobe Photoshop v 7.0 (Adobe, San Jose, CA).

RESULTS

P_0 is Localized to the Basolateral Surface of MDCK Cells

To determine whether P_0 contains targeting signals that can be interpreted by other polarized cells, full-length rat P_0 was expressed by transfection in MDCK cells. In several lines of stably transfected MDCK cells (Fig. 2), and in transiently transfected cultures (Fig. 3), full length myelin P_0 protein was consistently detected by confocal microscopy at the basolateral surfaces of polarized cells, but not at the apical surface. P_0 immunostaining did not overlap with GP135 (Fig. 2A), a marker of the apical membrane domain, but did colocalize with p58, a component of the basolateral membrane domain (Fig. 2B). Western blotting with P_0 antiserum detected an abundant ~28 kDa protein (Fig. 2C) in P_0-transfected cell lines that was not present in untransfected cells, confirming that the full-length P_0 protein was expressed.

In addition to basolateral plasma membrane labeling, P_0 was also detected in organelles in the apical cytoplasm. In myelinating Schwann cells, P_0 is a marker for the Golgi apparatus (Kidd et al., 1994; Trapp et al., 1981), but in MDCK cells, only a small amount of the intracellular P_0 staining colocalized with the Golgin97 protein (Fig. 2D). The majority of the intracellular P_0 was in LAMP-2-positive organelles (Figs. 2E,F), indicating that some P_0 was delivered to an internal lysosomal compartment. Little P_0 colocalized with transferrin-receptor or EEA1 staining for endosomes (data not shown). These data indicate that P_0 contains targeting information that is interpretable by the targeting mechanisms of MDCK cells. As P_0 accumulates in the basolateral membrane, targeting

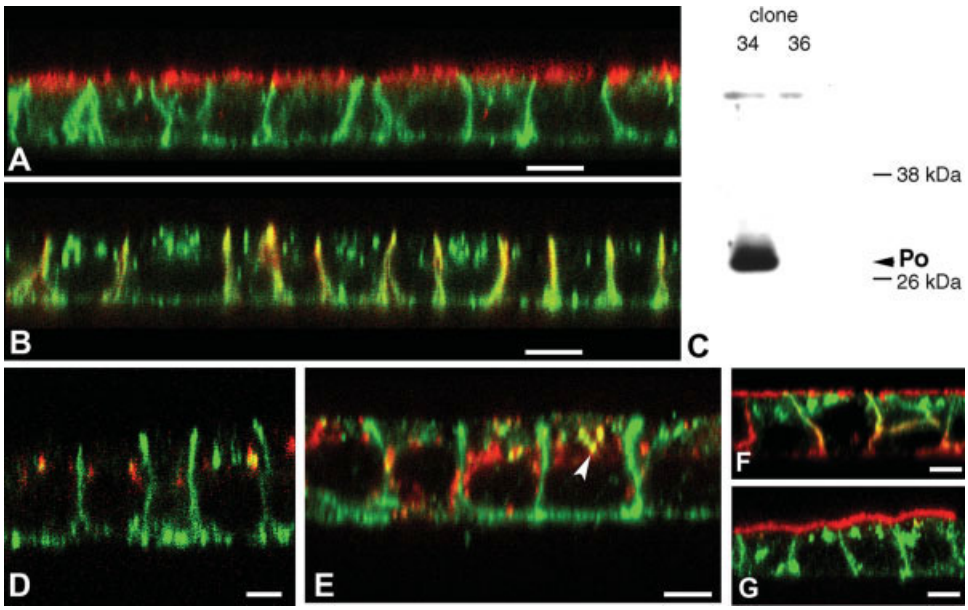

Fig. 2. P_0 is targeted to the basolateral surface of stably transfected MDCK cells. In *XZ* confocal images, P_0 immunostaining (green throughout) did not colocalize with apical marker GP135 (**A**, red) but was concentrated in basolateral membranes, which are immunostained for p58 (**B**, red). Western blotting (**C**) confirmed that full length P_0 was expressed in stably transfected MDCK clonal line 34 (shown in A, B; clone 36 was negative for P_0). Double-labeling for Golgin 97 (**D**, red) indicated minor staining of the Golgi apparatus for P_0; most P_0-positive internal organelles were LAMP-2-positive (**E**, red). In cotransfected cells, P_0 (**F**, green) and S-MAG (F, red) colocalized in the basolateral domain, with L-MAG (red, **G**) in both apical and basolateral membranes. In cells cotransfected with P_0 and S-MAG (G, red), the proteins has mutually exclusive distributions. A, B, D–G confocal *XZ* images. Scale bars 5 μm.

is not predominantly mediated by lipid rafts association, as raft-associated proteins are apically targeted in MDCK cells.

Homophilic trans-interactions between adjacent P_0-containing membranes occur in some P_0-transfected tissue culture lines (Filbin et al., 1990; Spiryda and Colman, 1998; Xu et al., 2001). In contrast, where P_0-expressing and nonexpressing MDCK cells apposed one another in transiently transfected cultures (Fig. 3A) or in mixed cultures of stably transfected and nontransfected cells, there was no obvious enrichment between the two P_0-expressing cells. No evidence of compact-myelin-like adhesion was observed between MDCK cell lateral membranes by electron microscopy (not shown), unlike CHO, HeLa, and L1 cells (Filbin et al., 1990; Spiryda and Colman, 1998; Xu et al., 2001). MDCK cell lateral membranes are normally separated by large intercellular gaps (~100 nm) except at junctional complexes, and this may prevent trans-interactions forming between P_0 molecules.

Cis-interactions between P_0 molecules have been proposed to result in liquid-crystal-like membrane microdomains that may exclude other proteins (Shapiro et al., 1996). P_0 and MAG have mutually exclusive distributions in Schwann cells (Trapp and Quarles, 1982, 1984), raising the possibility that P_0-containing membranes may exclude MAG. To test whether this occurred in MDCK cells, we coexpressed P_0 and either the large or small alternate splice forms of MAG, L-MAG, or S-MAG, and verified their expression by Western blot (not shown). As previously reported (Minuk and Braun, 1996), L-MAG was concentrated in both apical and basolateral membranes of transiently and stably transfected cells. When cotransfected stably (Fig. 2F) with P_0, P_0 and MAG distributions overlapped substantially in basolateral membranes, suggesting that P_0 did not exclude MAG, at least at the resolution of light microscopy. S-MAG accumulated in the apical membranes of both transiently and stably transfected MDCK cells. Coexpression of P_0 and S-MAG did not alter distributions of either protein (Fig. 2F).

P_0 Cytoplasmic Domain Contains Basolateral Targeting Information

Basolateral targeting signals are commonly peptide motifs in the cytoplasmic domain (Mostov et al., 2000, 2005; Yeaman et al., 1999). In an initial experiment, we investigated whether the P_0 cytoplasmic domain contained targeting information by introducing a stop codon to terminate translation immediately following R^{156}, which truncated the protein6 amino acids beyond the cytoplasmic face of the transmembrane domain (TMD, Fig. 1). In transient transfections, full length P_0 went to the basolateral surface (Fig. 3A), while the truncated protein was consistently located at the apical surface (Fig. 3B).

To better define the location(s) and number of basolateral signals, a series of stepwise truncations was introduced, deleting 15, 30, 45, and 60 amino acids from the C-terminal (Fig. 1; constructs Δ15, Δ30, Δ45, Δ60). Removal of the 15 C-terminal amino acids did not alter P_0 distribution (Figs. 3C,D), but deleting 30 amino acids produced a protein that localized entirely in the apical

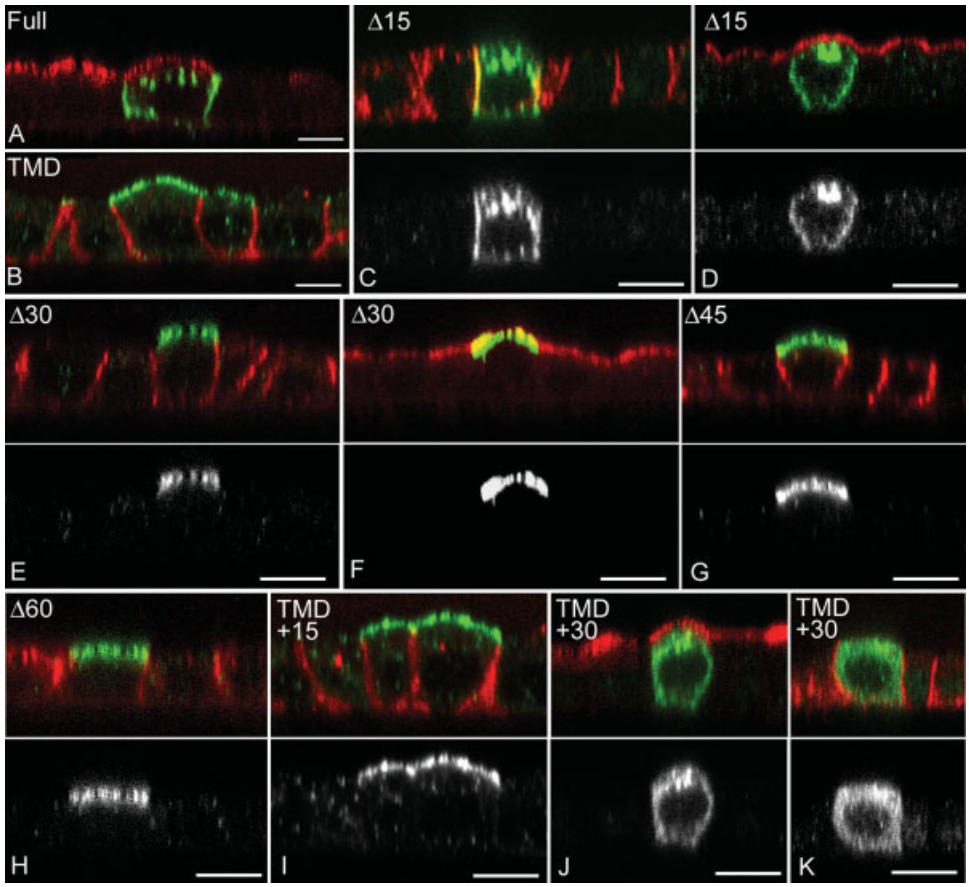

Fig. 3. The P_0 Cytoplasmic domain contains basolateral targeting signal(s). P_0 mutated proteins were expressed in transient transfections, and shown in green throughout. Red indicates apical GP135 (**A**, **D**, **F**, **J**) or basolateral p58 (**B**, **C**, **E**, **G**, **H**, **I**, **K**) staining; grayscale images (lower panels) show P_0 staining alone. As in stably transfected MDCK lines (Fig 2), full length P_0 (A) accumulates in the basolateral surface. P_0 lacking the cytoplasmic domain (B) was targeted to the apical surface. Removal of the C-terminal 15 amino acids did not alter P_0 distribution (C and D), but removal of 30 (E and F), 45 (G), and 60 (H) amino acids resulted in apical accumulation. Constructs with the entire cytoplasmic domain removed except the terminal 15 (TMD+15) or terminal 30 (TMD+30) amino acids were also expressed. TMD+15 proteins accumulated in the apical domain (I), while TMD+30 constructs were not expressed on the cell surface (J and K). All images are confocal XZ images. Scale bars 5 μm.

membrane (Figs. 3E,F), as did the Δ45 and Δ60 truncations (Figs. 3G,H). This result indicated that essential targeting information lay in the C-terminal 30 amino acids between V^{189} and S^{204}. Apical organelle staining was also consistently observed for the Δ15 construct, but lost with the longer truncations, suggesting that a signal in the Δ15–Δ30 region also targeted protein to these structures. The possibility of a redundant signal(s) in the Δ15 region was tested by fusing the terminal 15 amino acids to the TMD truncation C-terminal. This construct went to the apical surface (Fig. 3I), suggesting either that there were no signals in that region or they were not recognized in this conformation. A similar approach using the C-terminal 30 amino acids yielded a construct that appeared restricted to the cytoplasm (Figs. 3J,K). This result may be due to misfolding of the construct and subsequent RER retention. Alternatively, moving the C-terminal 30-mer adjacent to the plasma membrane may have altered trafficking of this protein so that surface accumulation did not occur.

Within the region between V^{189} and S^{204}, a YAML sequence at Y^{191} (Fig. 4A) conformed to the YxxΦ endocytosis/basolateral targeting consensus motif (where x is any amino acid and Φ is F/V/L/M/I; (Bonifacino and Traub, 2003; Marks et al., 1997). The YAML motif is highly conserved in vertebrate evolution (Fig. 4A), being identical in chickens, rodents, and humans, with only a conservative substitution in sharks; as discussed below, the teleosts were an exception. To investigate whether the YAML motif was functional and predominant, alanine was substituted for key amino acids in the sequence. As shown in Fig. 4B, a control protein consisting of full length P_0 or P_0 with a Y^{152} to A substitution went to the basolateral surface as expected. Y^{191} to A substitution yielded a protein found at both apical and basolateral domains (Figs. 4C,D). As tyrosine mutation disrupts the YxxΦ motif, this result suggested that another basolateral targeting motif within this region was also active, although not sufficient to drive basolateral targeting alone. An ML sequence serves as a leucine-based targeting signal in MHC Invariant Chain protein (Bremnes et al., 1994; Odorizzi et al., 1994), and resembles di-leucine-type basolateral targeting motifs (LL/I/M; Bonifacino and Traub, 2003; Marks et al., 1997). Conversion of YAML to AAAA resulted in apical accumulation of the P_0 protein (Fig. 4E), indicating that the ML motif was a second signal. Mutation of the M to A (YAAL) resulted in basolateral accumulation (Fig. 4F), indicating that the tyrosine-based motif alone was sufficient for basolateral targeting.

Concentration of P_0 in the apical LAMP2-positive organelles also depended on the presence of the YAML motif. P_0Δ15 mutants were found in these structures (Fig. 3C), but deletion of 30 or more amino acids from the C-terminal abolished targeting there (Figs. 3D–F). YAAL and AAML mutants (Fig. 4F,D respectively) also accumulated in these structures, but AAAA mutants did not (Fig. 4E), indicating that both YxxΦ motif and the ML motif were capable of

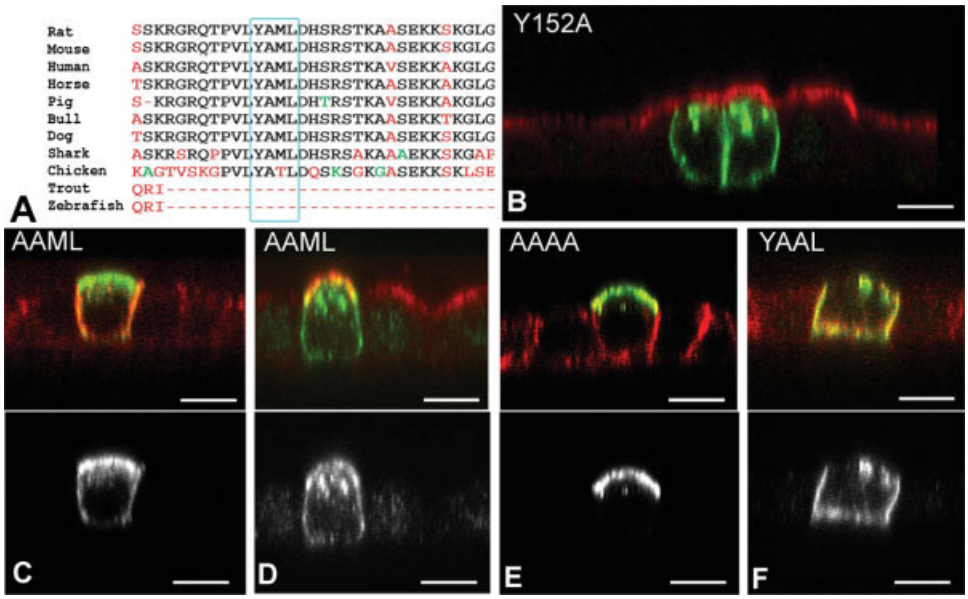

Fig. 4. The P_0 C-terminal sequence YAML is necessary for basolateral targeting and comprises two functional targeting motifs. The P_0 C-terminal sequence Y^{191}AML (**A**), conforms to the YxxΦ targeting consensus motif, and is highly conserved across species. Note that the YAML is embedded in an ITIM motif (consensus VxYxxL) and situated close to the RSTK PKC motif. The YAML motif was mutated and expressed in transiently transfected MDCK cells (P_0 shown in green throughout, red shows apical gp135 staining in **B** and **D**, and basolateral staining for p58 in **C**, **E**, and **F**. Lower panel grayscale images illustrate P_0 alone). P_0 with Y^{156}A mutation accumulated basolaterally (B). In contrast, Y^{191}A substituted P_0 (AAML) was detected in both apical and basolateral membranes (C and D). When the YAML sequence was converted to AAAA (E), P_0 was only detected apically. YAAL-mutants were only detected basolaterally (**G**). Confocal *XZ* images; scale bars 5 μm. (Accession numbers (A) (NP_058723.1, [Rattus norvegicus]; NP_032649.1[Mus musculus]; P25189 [human]; AAQ55549.1 [Equus caballus]; CAI45377.1[Sus scrofa]; XP_587311.1 [Bos taurus]; XP_545771.1 [Canis familiaris]; CAB37865.1 [Heterodontus francisci]; A61087 [gallus gallus]; AAB34399.1 IP1 [Salmo sp.]; CAD32961.1 [Danio rerio])).

directing P_0 for inclusion in these structures. Thus accumulation in these structures likely represents a pathway of P_0 trafficking and not simply the result of P_0 aggregation due to aberrant overexpression.

C-Terminal Tyrosine Motif Targets EGFP-Based P_0 Constructs

Proteins lacking any targeting information may be expected to accumulate in both apical and basolateral MDCK cell surfaces, but the P_0 constructs lacking the YAML sequence accumulated at the apical surface. This suggests that the P_0 extracellular domain may have contained secondary apical signals that were active in the absence of the primary YAML targeting sequences. To test for these effects, we excised the P_0 extracellular domain between Y^4 and E^{119}, and replaced them with EGFP (Fig. 1). This generated a polypeptide with the P_0 signal peptide, the initial 4 amino acids of mature P_0, EGFP, the last 6 amino acids of the P_0 extracellular domain followed by the P_0 transmembrane and cytoplasmic domains.

Expression of this construct provided sufficient EGFP fluorescence for direct confocal imaging (Fig. 5), although the fluorescence signal intensity was reduced compared with cytosolic expression of native EGFP (not shown). Immunostaining for EGFP and P_0 negated the possibility that nonfluorescent P_0-EGFP was accumulating elsewhere undetected by EGFP fluorescence imaging. Results with P_0-EGFP constructs were similar to those obtained with the P_0 extracellular domain. The construct with the native P_0 cytoplasmic domain accumulated in the basolateral membrane (Fig. 5A), as did the Δ15 deletion (Fig. 5B). The Δ30 and Δ60 constructs were predominantly apical, although unlike those with the P_0 extracellular domain, some protein was also observed in the basolateral membranes (Figs. 5C,D). Mutations of the tyrosine motif to AAML resulted in mixed apical and basolateral localization (Fig. 5E), as observed previously for P_0. Constructs with the YAML mutated to AAAA accumulated in the apical surface, although minor basolateral fluorescence was also detected (Fig. 5F). YAAL-containing protein was concentrated at the basolateral surface (Fig. 5G). These results confirm that the YAML sequence is the predominant targeting signal, but indicate that the P_0 extracellular domain contains signals not present in the P_0-EGFP that direct P_0 to the apical surface in the absence of the tyrosine motif.

DISCUSSION

We show here for the first time that P_0 contains a unique dual-motif targeting signal that contains both tyrosine- and leucine-based elements, as part of a hierarchy of targeting signals that are recognized by the sorting machinery in MDCK cells. The predominant targeting signal is the YxxΦ motif, which is necessary and sufficient for basolateral accumulation of P_0. Superim-

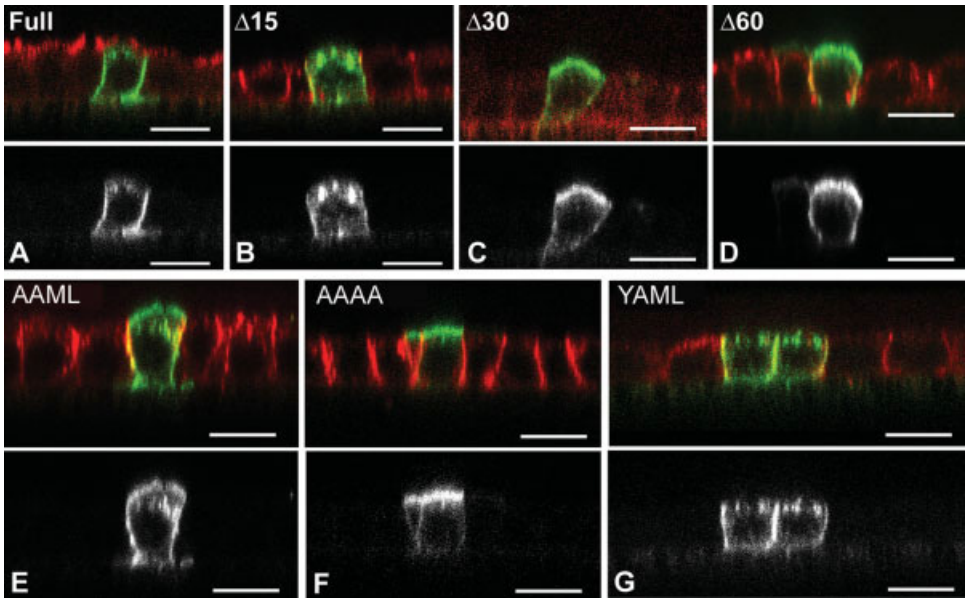

Fig. 5. EGFP substitution for the P_0 extracellular domain. Transiently transfected into MDCK cells, P_0-EGFP constructs emitted sufficient fluorescence for imaging by confocal microscopy (green throughout). Full length P_0-EGFP accumulated in the basolateral membrane (**A**, apical GP135 immunostaining shown in red). Deletion of 15 amino acids from the C-terminal did not alter this (B, red shows p58 in **B**–**G**), but deletion of 30 (C) and 60 (D) amino acids resulted in detection of P_0-EGFP at both apical and basolateral surfaces. Alanine substitutions for Y^{191} (E) also resulted in accumulation at both surfaces. When both Y^{191} and M^{193} were mutated (F), most of the staining was detected at the apical surface, although minor staining was also detected in the basolateral membrane. M^{193} to A substitution alone resulted in basolateral detection. Confocal *XZ* images. Scale bar 5 μm.

posed on the same sequence is a subordinate leucine-based basolateral-targeting motif, ML. The P_0 extracellular domain also contains apical targeting information, which contributes to P_0 localization if the tyrosine-based signal is absent. P_0 localization in MDCK cells was not dependent on raft associations, which direct proteins to the apical surface (Barman and Nayak, 2000; Benting et al., 1999; Weimbs et al., 1997), and P_0 self-association in trans also appeared unnecessary. Possible cis-associations of P_0 did not exclude MAG from membranes. These results provide important candidate signals for studies of P_0 targeting in myelination and in dysmyelinating diseases.

In MDCK cells, the Y^{191}AML region was the primary means of targeting P_0 to the cell surface. Consensus pattern-matching had identified both P_0 tyrosine and leucine motifs as potential targeting components, but in many proteins, potential targeting motifs are buried within folded regions or insufficiently close to the C-terminal to permit interaction with recognition molecules. Our results indicate that the P_0 YAML is accessible to interact with cellular targeting machinery. Tyrosine-based motifs are recognized by μ subunits of the clathrin adapter protein (AP) complexes (Bonifacino and Traub, 2003; Mostov et al., 2000; Owen and Evans, 1998), which incorporate the targeted protein into budding clathrin-coated vesicles on the TGN or during recycling to/from the cell surface (Bonifacino and Traub, 2003; Mostov et al., 2000). We envisage that in Schwann cells, AP-clathrin interactions may be involved in the sorting of P_0 into unique carrier vesicles, which occurs at the TGN (Trapp et al., 1995). To our knowledge, the direct superimposition of tyrosine and leucine motifs has not been described previously, although partial overlaps of tyrosine and leucine motifs occurs in CD1d (Rodionov et al., 2000) and adjacent tyrosine and leucine-based motifs have been described in tyrosinase (Simmen et al., 1999). Leucine-based motifs may be recognized by several adaptor-complex proteins. For stochiometric reasons, it seems unlikely that both motifs are recognized simultaneously, although the possibility that Schwann cells express unusual AP complexes that recognize both cannot be discounted. In other proteins, close proximity of tyrosine and leucine motifs promotes endocytosis and lysosomal delivery as well as basolateral delivery. Although both tyrosine and leucine motifs may direct proteins to endosomal compartments, in Schwann cells, P_0 is not normally found in endosomes, though it does accumulate there in P_0-overexpressing transgenics (Yin et al., 2000), and to a minor extent in dedifferentiated Schwann cells (Poduslo and Windebank, 1995). In MDCK cells, in addition to basolateral targeting, some P_0 was delivered to LAMP-2-positive organelles when either tyrosine or leucine signals were present. Internal accumulation of P_0 is not observed in normal myelinating Schwann cells, but after microtubule disruption (Trapp et al., 1995) and possibly during myelin degradation in Wallerian degeneration, the YAML motif may function as an endocytosis/lysosomal targeting motif.

In humans, point mutations that specifically affect the Y^{191} in P_0 have not been reported, but several mutations cause C-terminal truncations that delete or disrupt the YAML motif and result in severe, early onset neuropathies (Kamholz et al., 2000; Shy et al., 2004). These include Q^{186}X (Mandich et al., 1999; Shy et al., 2004), A^{159}frameshift (Tachi et al., 1998), and A^{192}frameshift

(Rautenstrauss et al., 1994). Explanations for the resultant pathology have focused on the importance of downstream PKC-binding sites and phosphorylation sites, which are necessary for P_0 adhesion in cultured cells (Xu et al., 2001). Our data here support the possibility that P_0 mistargeting may also contribute to P_0 insufficiency in compact myelin and ineffective remyelination in these patients. In P_0 overexpressing transgenic mice, P_0 mistargeting to the developing mesaxon occurs (Yin et al., 2000) and inhibits myelin spiral growth and compact myelin formation (Wrabetz et al., 2000; Yin et al., 2000). In published patient biopsies (Mandich et al., 1999), disability appeared to result primarily from demyelination rather than arrested myelination; as P_0 mutations are heterozygous in humans, sufficient wild type P_0 may be available to initially form myelin. Also as C-terminal truncations effect P_0 adhesion, mistargeted P_0 in human Schwann cells may not be capable of generating the mesaxonal adhesions seen in P_0 overexpressing mouse (Yin et al., 2000). The extent to which P_0 mistargeting interferes with initial myelination and promotes demyelination in these patients remain to be investigated. Based on our data using truncated P_0 (Δ30, Δ45, Δ60), that P_0 C-terminal truncation mutations do not inherently cause an unfolded protein endoplasmic reticulum response; only one construct in our hands was retained in the MDCK cell cytoplasm, and that involved a large internal deletion within the C-terminal.

The YAML sequence is part of a larger immunoreceptor tyrosine-based inhibitory motif (ITIM; consensus VxYxxL; (Bolland and Ravetch, 1999; Burshtyn et al., 1999; see Fig. 4), which is an important inhibitory signaling module found in several immune receptors, including the Fc receptor, PECAM, and CD5 (Billadeau and Leibson, 2002; Bolland and Ravetch, 1999). By definition, ITIMs also conform to the YxxΦ consensus sequence for targeting motifs. Activation of the P_0 ITIM through phosphorylation of Y^{191} has been reported during early postnatal development (Iyer et al., 2000; Xu et al., 2000) and putative signaling proteins that bind to the ITIM have been reported (Xu et al., 2000). Phosphorylation has reciprocal effects on ITIM and YxxΦ signals, since phosphorylation inactivates AP binding to YxxΦ motifs (Anderson et al., 2005), and binding of proteins to the ITIM motif would also presumably block any trafficking role of this domain. The functional significance of this for P_0 in myelination is unclear, though it is possible to envisage a scenario in which YAML serves in TGN sorting and then is inactivated by phosphorylation, which prevents subsequent activity as an endocytosis signal.

The YAML sequence is remarkably conserved in evolution (Fig. 4A), as is the entire P_0 molecule. The YAML signal is absolutely conserved in higher vertebrates (Fig. 4A) with only a minor substitution ($M^{193}T$) in elasmobranchs, in which myelin is first seen evolutionarily. In lower vertebrates (Yoshida and Colman, 1996), P_0 is expressed in oligodendrocytes, and the YAML motif may also serve in oligodendrocyte P_0 targeting. Mouse oligodendrocytes retain the ability to correctly target transgenically expressed P_0 to compact myelin membranes in oligodendrocytes (Yin et al., 2006), suggesting that the targeting mechanisms may be conserved throughout vertebrate oligodendrocyte evolution, even though P_0 is no longer a CNS protein. The major exception to P_0 conservation is in the bony fishes where the P_0 cytoplasmic tail diverges greatly from other vertebrates (Fig. 4A). Not only is the YAML motif lost, but other domains believed necessary for adhesion, such as the PKC motif, are also deleted. The resulting protein incorporates many of the disease-promoting features of CMT-1B P_0 mutations (Kamholz et al., 2000; Shy et al., 2004). Myelin membrane assembly in teleosts is thus likely to follow a different course from other vertebrates, and may be mediated by proteins not found in mammals, such as the 36 kDa protein (Morris et al., 2004).

Our results identified a hierarchy of targeting signals in P_0, but it remains to be determined whether Schwann cells interpret these signals in the same precedence as MDCK cells. In addition to the YAML region, the ectodomain contained an apical signal, that may have been post-translational carbohydrate addition, which can mediate apical targeting in MDCK cells. Palmitoylation can also mediate protein targeting, and palmitoylation of C^{153} is important in P_0 adhesion in CHO cells (Gao et al., 2000), but was not utilized by MDCK cells as a primary means of P_0 targeting. P_0-homotypic adhesion did not appear to be a major factor in MDCK cell targeting, as P_0–P_0 trans-interaction between cells was not essential for basolateral localization and substitution of the adhesive P_0 ectodomain with EGFP did not alter targeting. Differences in targeting between Schwann cells and MDCK cells are obviously important. P_0 and MAL (Cheong et al., 1999) target to different MDCK cell surfaces, but are both found in compact PNS myelin (Schaeren-Wiemers et al., 1995). L-MAG and P_0 at least partially overlap in distribution in MDCK cells (Minuk and Braun, 1996) (Fig. 2), but have mutually exclusive distributions in Schwann cells (Trapp and Quarles, 1982). Myelinating Schwann cells have at least five distinct membrane domains (Arroyo and Scherer, 2000; Trapp et al., 2004), compared with two in MDCK cells, and presumably use a combination of targeting signals to specify delivery to each membrane domain. Discovering which signals combine to effect transport to each domain provides a major challenge for the future.

ACKNOWLEDGMENTS

We thank Peter Braun and David Colman for cDNAs, and Rosa Yacubova for assistance in preparing figures.

REFERENCES

Anderson E, Maday S, Sfakianos J, Hull M, Winckler B, Sheff D, Folsch H, Mellman I. 2005. Transcytosis of NgCAM in epithelial cells reflects differential signal recognition on the endocytic and secretory pathways. J Cell Biol 170:595–605.

Arroyo EJ, Scherer SS. 2000. On the molecular architecture of myelinated fibers. Histochem Cell Biol 113:1–18.

Barman S, Nayak DP. 2000. Analysis of the transmembrane domain of influenza virus neuraminidase, a type II transmembrane glycoprotein, for apical sorting and raft association. J Virol 74:6538–6545.
Benting JH, Rietveld AG, Simons K. 1999. N-Glycans mediate the apical sorting of a GPI-anchored, raft-associated protein in Madin-Darby canine kidney cells. J Cell Biol 146:313–320.
Billadeau DD, Leibson PJ. 2002. ITAMs versus ITIMs: Striking a balance during cell regulation. J Clin Invest 109:161–168.
Bö L, Quarles RH, Fujita N, Bartoszewicz Z, Sato S, Trapp BD. 1995. Endocytic depletion of L-MAG from CNS myelin in quaking mice. J Cell Biol 131:1811–1820.
Bolland S, Ravetch JV. 1999. Inhibitory pathways triggered by ITIM-containing receptors. Adv Immunol 72:149–177.
Bonifacino JS, Traub LM. 2003. Signals for sorting of transmembrane proteins to endosomes and lysosomes. Annu Rev Biochem 72:395–447.
Bremnes B, Madsen T, Gedde-Dahl M, Bakke O. 1994. An LI, ML motif in the cytoplasmic tail of the MHC-associated invariant chain mediate rapid internalization. J Cell Sci 107:2021–2032.
Burshtyn DN, Lam AS, Weston M, Gupta N, Warmerdam PA, Long EO. 1999. Conserved residues amino-terminal of cytoplasmic tyrosines contribute to the SHP-1-mediated inhibitory function of killer cell Ig-like receptors. J Immunol 162:897–902.
Cheong KH, Zacchetti D, Schneeberger EE, Simons K. 1999. VIP17/MAL, a lipid raft-associated protein, is involved in apical transport in MDCK cells. Proc Natl Acad Sci USA 96:6241–6248.
de Hoop MJ, Dotti CG. 1993. Membrane traffic in polarized neurons in culture. J Cell Sci 17 (Suppl):85–92.
D'Urso D, Brophy PJ, Staugaitis SM, Gillespie CS, Frey AB, Stempak JG, Colman DR. 1990. Protein zero of peripheral nerve myelin: Biosynthesis, membrane insertion, and evidence for homotypic interaction. Neuron 2:449–460.
Feltri ML, Graus PD, Previtali SC, Nodari A, Migliavacca B, Cassetti A, Littlewood-Evans A, Reichardt LF, Messing A, Quattrini A, Mueller U, Wrabetz L. 2002. Conditional disruption of β-1 integrin in Schwann cells impedes interactions with axons. J Cell Biol 156:199–209.
Filbin MT, Walsh FS, Trapp BD, Pizzey JA, Tennekoon GI. 1990. The role of myelin P_0 protein as a homophilic adhesion molecule. Nature 344:871,872.
Gao Y, Li W, Filbin MT. 2000. Acylation of myelin Po protein is required for adhesion. J Neurosci Res 60:704–713.
Giese KP, Martini R, Lemke G, Soriano P, Schachner M. 1992. Mouse P_0 gene disruption leads to hypomyelination, abnormal expression of recognition molecules, and degeneration of myelin and axons. Cell 71565–576.
Heath JW, Inuzuka T, Quarles RH, Trapp BD. 1991. Distribution of P_0 protein and the myelin-associated glycoprotein in peripheral nerves from Trembler mice. J Neurocytol 20:439–449.
Inouye H, Tsuruta H, Sedzik J, Uyemura K, Kirschner DA. 1999. Tetrameric assembly of full-sequence protein zero myelin glycoprotein by synchrotron x-ray scattering. Biophys J 76:423–437.
Iyer S, Bianchi R, Eichberg J. 2000. Tyrosine phosphorylation of PNS myelin P(0) occurs in the cytoplasmic domain and is maximal during early development. J Neurochem 75:347–354.
Kamholz J, Menichella D, Jani A, Garbern J, Lewis RA, Krajewski KM, Lilien J, Scherer SS, Shy ME. 2000. Charcot-Marie-Tooth disease type 1: Molecular pathogenesis to gene therapy. Brain 123:222–233.
Kidd GJ, Andrews SB, Trapp BD. 1994. Organization of microtubules in myelinating Schwann cells. J Neurocytol 23:801–810.
Kidd GJ, Andrews SB, Trapp BD. 1996. Axons regulate the distribution of Schwann cell microtubules. J Neurosci 16:946–954.
Kroepfl JF, Gardinier MV. 2001. Identification of a basolateral membrane targeting signal within the cytoplasmic domain of myelin/oligodendrocyte glycoprotein. J Neurochem 77:1301–1309.
Low SH, Chapin SJ, Weimbs T, Komuves LG, Bennett MK, Mostov KE. 1996. Differential localization of syntaxin isoforms in polarized Madin-Darby canine kidney cells. Mol Biol Cell 7:2007–2018.
Low SH, Chapin SJ, Wimmer C, Whiteheart SW, Komuves LG, Mostov KE, Weimbs T. 1998. The SNARE machinery is involved in apical plasma membrane trafficking in MDCK cells. J Cell Biol 141:1503–1513.
Mandich P, Mancardi GL, Varese A, Soriani S, Di ME, Bellone E, Bado M, Gross L, Windebank AJ, Ajmar F, Schenone A. 1999. Congenital hypomyelination due to myelin protein zero Q215X mutation. Ann Neurol 45:676–678.
Marks MS, Ohno H, Kirchhausen T, Bonifacino JS. 1997. Protein sorting by tyrosine-based signals: Adapting to the Ys and wherefores. Trends Cell Biol 7:124–128.
Matter K, Mellman I. 1994. Mechanisms of cell polarity: Sorting and transport in epithelial cells. Curr Opin Cell Biol 6:545–554.
Minuk J, Braun PE. 1996. Differential intracellular sorting of the myelin-associated glycoprotein isoforms. J Neurosci Res 44:411–420.
Morris JK, Willard BB, Yin X, Jeserich G, Kinter M, Trapp BD. 2004. The 36K protein of zebrafish CNS myelin is a short-chain dehydrogenase. Glia 45:378–391.
Mostov K, Su T, ter Beest M. 2003. Polarized epithelial membrane traffic: Conservation and plasticity. Nat Cell Biol 5:287–293.
Mostov KE, Verges M, Altschuler Y. 2000. Membrane traffic in polarized epithelial cells. Curr Opin Cell Biol 12:483–490.
Nelson WJ, Yeaman C. 2001. Protein trafficking in the exocytic pathway of polarized epithelial cells. Trends Cell Biol 11:483–486.
Norton WT, Cammer W. 1984. Isolation and characterization of myelin. In: Morell P, editor. Myelin. New York: Plenum. pp 146–196.
Odorizzi CG, Trowbridge IS, Xue L, Hopkins CR, Davis CD, Collawn JF. 1994. Sorting signals in the MHC class II invariant chain cytoplasmic tail and transmembrane region determine trafficking to an endocytic processing compartment. J Cell Biol 126:317–330.
Owen DJ, Evans PR. 1998. A structural explanation for the recognition of tyrosine-based endocytotic signals. Science 282:1327–1332.
Pedraza L, Huang JK, Colman DR. 2001. Organizing principles of the axoglial apparatus. Neuron 30:335–344.
Poduslo JF, Windebank AJ. 1995. Differentiation-specific regulation of Schwann cell expression of the major myelin glycoprotein. Proc Natl Acad Sci USA 82:5987–5991.
Rautenstrauss B, Nelis E, Grehl H, Pfeiffer RA, Van BC. 1994. Identification of a de novo insertional mutation in P0 in a patient with a Dejerine-Sottas syndrome (DSS) phenotype. Hum Mol Genet 3:1701, 1702.
Rodionov DG, Nordeng TW, Kongsvik TL, Bakke O. 2000. The cytoplasmic tail of CD1d contains two overlapping basolateral sorting signals. J Biol Chem 275:8279–8282.
Schaeren-Wiemers N, Valenzuela DM, Frank M, Schwab ME. 1995. Characterization of a rat gene, rMAL, encoding a protein with four hydrophobic domains in central and peripheral myelin. J Neurosci 15: 5753–5764.
Scherer S. 1999. Axonal pathology in demyelinating diseases. Ann Neurol 45:6–7.
Shapiro L, Doyle JP, Hensley P, Colman DR, Hendrickson WA. 1996. Crystal structure of the extracellular domain from P_0, the major structural protein of peripheral nerve myelin. Neuron 17:435–449.
Sherman DL, Brophy PJ. 2005. Mechanisms of axon ensheathment and myelin growth. Nat Rev Neurosci 6:683–690.
Sherman DL, Fabrizi C, Gillespie CS, Brophy PJ. 2001. Specific disruption of a Schwann cell dystrophin-related protein complex in a demyelinating neuropathy. Neuron 30:677–687.
Shy ME, Jani A, Krajewski K, Grandis M, Lewis RA, Li J, Shy RR, Balsamo J, Lilien J, Garbern JY, Kamholz J. 2004. Phenotypic clustering in MPZ mutations. Brain 127:371–384.
Silverman MA, Peck R, Glover G, He C, Carlin C, Banker G. 2005. Motifs that mediate dendritic targeting in hippocampal neurons: A comparison with basolateral targeting signals. Mol Cell Neurosci 29: 173–180.
Simmen T, Schmidt A, Hunziker W, Beermann F. 1999. The tyrosinase tail mediates sorting to the lysosomal compartment in MDCK cells via a di-leucine and a tyrosine-based signal. J Cell Sci 112:45–53.
Spiryda LB, Colman DR. 1998. Protein zero, a myelin IgCAM, induces physiologically operative tight junctions in nonadhesive carcinoma cells. J Neurosci Res 54:282–288.
Tachi N, Kozuka N, Ohya K, Chiba S, Yamashita S. 1998. A small direct tandem duplication of the myelin protein zero gene in a patient with Dejerine-Sottas disease phenotype. J Neurol Sci 156:167–171.
Thomas PK, Barthold C-H, Ochoa J. 1993. Microscopic anatomy of the peripheral nervous system. In: Dyck PJ, Thomas PK, Griffin JW, Low PA, Poduslo JF, editors. Peripheral neuropathy. Philadelphia: W.B. Saunders. pp 28–98.
Trapp BD, Itoyama Y, Sternberger NH, Quarles RH, Webster H. 1981. Immunocytochemical localization of P_0 protein in Golgi complex membranes and myelin of developing rat Schwann cells. J Cell Biol 90:1–6.
Trapp BD, Kidd GJ. 2004. Structure of the myelinated axon. In: Lazzarini R, editor. Myelin biology and disorders. New York: Elsevier. pp 3–25.
Trapp BD, Kidd GJ, Hauer PE, Mulrenin E, Haney C, Andrews SB. 1995. Polarization of myelinating Schwann cell surface membranes: Role of microtubules and the trans-Golgi network. J Neurosci 15:1797–1807.
Trapp BD, Pfeiffer SE, Anitei M, Kidd GJ. 2004. Cell biology of myelin assembly. In: Lazzarini R, editor. Myelin biology and disorders. New York: Elsevier. pp 29–55.
Trapp BD, Quarles RH. 1982. Presence of the myelin-associated glycoprotein correlates with alterations in the periodicity of peripheral myelin. J Cell Biol 92:877–882.
Trapp BD, Quarles RH. 1984. Immunocytochemical localization of the myelin-associated glycoprotein: Fact or artifact? J Neuroimmunol 6: 231–249.
Valentijn LJ, Bolhuis PA, Zorn I, Hoogendijk JE, van Laack HL, Hensels GW, Stanton VP Jr, Housman DE, Fischbeck KH, Ross DA, Nicholson GA, Meershoek EJ, Dauwerse HG, van Ommen G-JB, Baas F. 1992. The peripheral myelin gene PMP-22/GAS-3 is duplicated in Charcot-Marie-Tooth disease type 1A. Nat Genet 1:166–170.

Weimbs T, Low SH, Chapin SJ, Mostov KE. 1997. Apical targeting in polarized epithelial cells: There's more afloat than rafts. Trends Cell Biol 7:393–399.

Wrabetz L, Feltri ML, Klugmann M, Scherer SS. 2004. Inherited neuropathies: Clinical, genetic, and biological features. In: Lazzarini R, editor. Myelin biology and disorders. New York: Elsevier. pp 905–952.

Wrabetz L, Feltri ML, Quattrini A, Imperiale D, Previtali S, D'antonio M, Martini R, Yin X, Trapp BD, Zhou L, Chiu SY, Messing A. 2000. P0 glycoprotein overexpression causes congenital hypomyelination of peripheral nerves. J Cell Biol 148:1021–1034.

Xu W, Shy M, Kamholz J, Elferink G, Xu G, Lilien J, Balsamo J. 2001. Mutations in the cytoplasmic domain of P0 reveal a role for PKC-mediated phosphorylation in adhesion and myelination. J Cell Biol 155:439–445.

Xu M, Zhao R, Sui X, Xu F, Zhao ZJ. 2000. Tyrosine phosphorylation of myelin P(0) and its implication in signal transduction. Biochem Biophys Res Commun 267:820–825.

Yeaman C, Grindstaff KK, Nelson WJ. 1999. New perspectives on mechanisms involved in generating epithelial cell polarity. Physiol Rev 79:73–98.

Yin X, Crawford TO, Griffin JW, Tu P-H, Lee VMY, Li C, Roder J, Trapp BD. 1998. Myelin-associated glycoprotein is a myelin signal that modulates the caliber of myelinated axons. J Neurosci 18:1953–1962.

Yin X, Kidd GJ, Wrabetz L, Feltri ML, Messing A, Trapp BD. 2000. Schwann cell myelination requires timely and precise targeting of P0 protein. J Cell Biol 148:1009–1020.

Yin X, Peterson J, Gravel M, Braun PE, Trapp BD. 1997. CNP overexpression induces aberrant oligodendrocyte membranes and inhibits MBP accumulation and myelin compaction. J Neurosci Res 50:238–247.

Yin X, Baek RC, Kirschner DA, Peterson A, Fujii Y, Nave K-A, Macklin WB, Trapp BD. 2006. Evolution of a neuroprotective function of central nervous system myelin. J Cell Biol 172:469–478.

Yoshida M, Colman DR. 1996. Parallel evolution and coexpression of the proteolipid proteins and protein zero in vertebrate myelin. Neuron 16:1115–1126.

Zhang K, Filbin MT. 1998. Myelin P_0 protein mutated at Cys21 has a dominant-negative effect on adhesion of wild type P_0. J Neurosci Res 53:1–6.